Standard Article

International Journal of ENGINE RESEARCH

International J of Engine Research
1–13

DOI: 10.1177/14680874211055580
journals.sagepub.com/home/jer
SAGE

Effects of differential pressure measurement characteristics on high pressure-EGR estimation error in SI-engines

Sumanth Reddy Dadam, Imtiaz Ali, Di Zhu and Vivek Kumar

Abstract

With proper control, exhaust gas recirculation (EGR) can be used for knock mitigation in SI engines, enabling fuel economy improvements through more optimal combustion phasing and lower fuel-enrichment at high loads. Due to significant pressure pulsations across the EGR valve, estimating the mass flow rates at transient and reversing flows across the valve can be challenging. Many systems utilize the pressure drop across a restriction in a flow path as an indication of mass flow. In automotive applications, the measurement of the pressure drop is accomplished by the use of a delta pressure sensor and the pressure drop mechanism could be a sharp edge orifice or other restrictions such as a valve opening. This technique works well for steady-state flow; however, if pressure fluctuations exist, especially at higher frequencies, this method of measuring mass flow can have large errors. The accuracy of EGR mass flow estimation based on a pressure differential (ΔP) measurement and the steady compressible flow orifice equation is investigated for various ΔP sensor frequencies and sampling rates on Ford 3.5L V6 GTDI and 2.3L I4 GTDI engines. This paper identifies the two major contributors of the error are the long length of the gauge lines and the close location of the downstream tap. The long length of the gauge line results in resonances at low frequency which affects the sensor performance. When the downstream tap is placed too close to the orifice, the accuracy of sensor reading is reduced. The proposed solution suggests keeping the gauge line as short as possible and the downstream tap at least two diameters away from the orifice and using a high-speed sensor. The result from engine testing shows a great improvement in the measurement accuracy by 43%. It is demonstrated that using a slow responding sensor with a low sample rate leads to erroneous mass flow calculation when significant pressure pulsations exist. A minimum of 1 kHz sample rate is needed to increase the accuracy of the EGR estimate within $\pm 1\%$.

Keywords

High pressure EGR, SI engines, fuel economy, flow measurement, pressure sensors

Date received: 19 June 2021; accepted: 23 September 2021

Introduction

In the automotive industry, Exhaust Gas Recirculation (EGR) is often implemented as a method for reducing the combustion temperature and pumping losses. An example of a low-pressure EGR (LPEGR) and a high-pressure EGR system are shown in Figure 1(a) and (b). EGR involves taking some portion of exhaust gas and rerouting it toward the intake where it mixes with fresh air and is then ingested into the engine. EGR is actively cooled by a coolant-fed heat exchanger to minimize the temperature rise of the air/EGR mixture that is inducted into the engine. The motive force for the EGR to flow from the exhaust into the intake is a pressure differential between the intake and the exhaust system. This differential pressure can be actively controlled by a secondary throttle Air Intake System (AIS) throttle in the intake system for turbocharged engines as in the LPEGR example or it can be a natural pressure differential in which the exhaust pressure is higher than the intake pressure as in the HPEGR example. During combustion, energy is used up to increase the

Powertrain Research and Advanced Engineering, Ford Motor Company, Dearborn, MI, USA

Corresponding author:
Sumanth Reddy Dadam, Powertrain Research and Advanced Engineering, Ford Motor Company, 20000 Rotunda Drive, Dearborn, MI 48121, USA.
Email: sdadam@ford.com

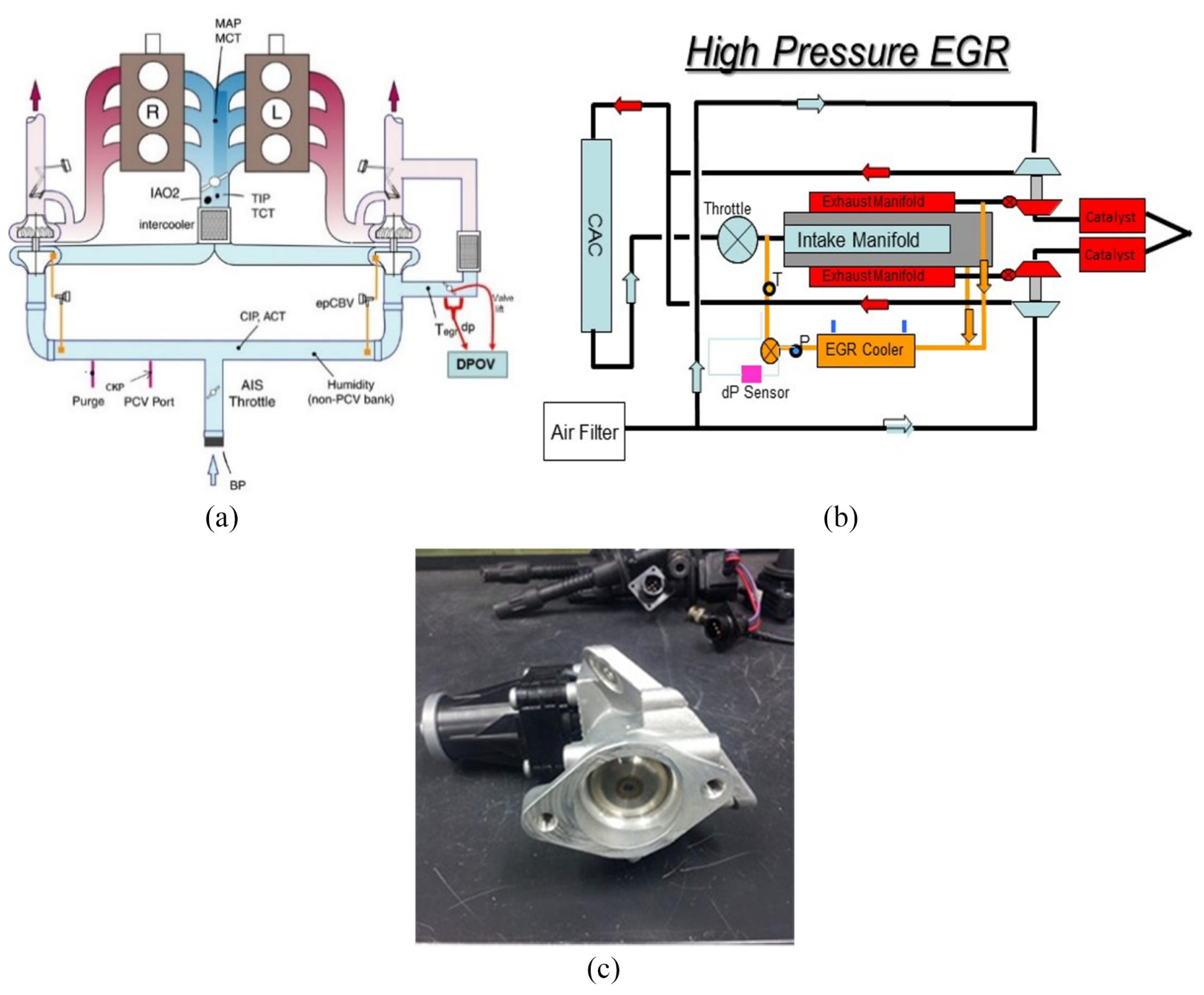

Figure 1. (a) Schematic of a low-pressure EGR (LPEGR) system. Hardware components consist of AIS throttle, EGR cooler, EGR valve and delta pressure sensor, (b) schematic of a high-pressure EGR (HPEGR) system. Hardware components consist of an EGR cooler, EGR valve and delta pressure sensor, and (c) EGR poppet valve used on HP EGR system.

temperature of the non-volatile EGR gas which reduces the combustion chamber temperature resulting in less heat loss to cylinder walls and more combustion energy going toward producing useful work. The temperature-reducing effects of EGR also create a more knock tolerant condition for engine operation. The amount of EGR is scheduled by the Engine Control Module (ECM) and depends on the engine operating conditions. To meet the torque request from the engine, a given quantity of air must be delivered to the engine and the requisite amount of fuel must be mixed in to satisfy the requested air-fuel ratio. Because a scheduled amount of EGR displaces air, the throttle must open more to compensate for the displaced air to meet the torque and fueling demand. This has the effect of reducing pumping losses. Henceforth, in automotive applications, the accurate flow rate measurement of EGR is important.

Though knock propensity is increased with the use of internal exhaust gas recirculation (EGR),[1] cooled external EGR reduces both knock tendency and exhaust gas temperatures.[2–4] Hence, the use of external EGR can potentially improve the engine efficiency at high loads by allowing more optimal combustion phasing and less fuel enrichment. Alternatively, it can permit more aggressive downsizing, further shifting the engine operation into more efficient regions.[4] In particular, Zhong et al.[5] reported that low pressure (LP) EGR is more suitable for the low rpm range whereas the high pressure (HP) configuration is the better alternative at higher RPMS. However, in either case, excessive amounts of EGR result in combustion instabilities.[5] The ability to accurately estimate and control the fraction of external EGR is therefore crucial to avoid the misfire and partial burn regions that can destroy any potential fuel economy gains with external EGR. In previous works, Liu and Pfeiffer,[6] looked at EGR mass-flow measurement accuracy in the presence of significant pressure pulsations on LP-EGR and recommended keeping the average pressure differential (ΔP)

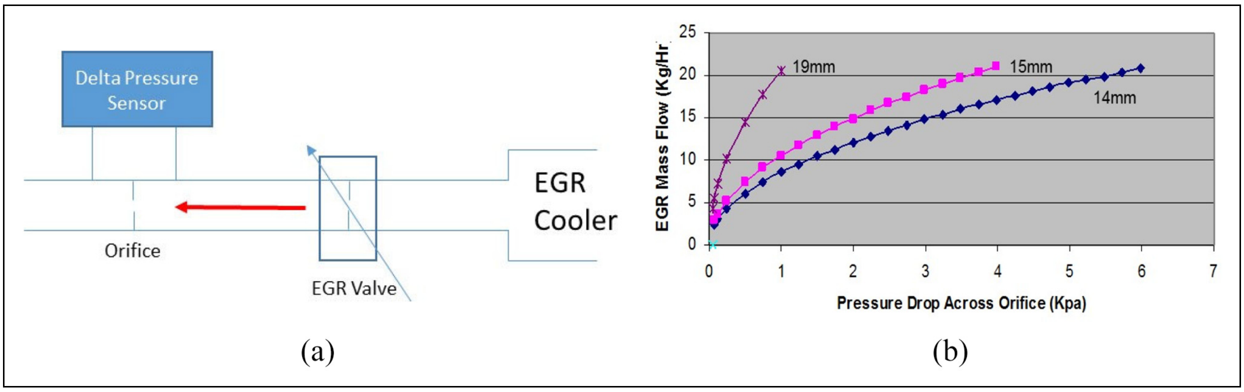

Figure 2. (a) Schematic of placement of orifice and EGR valve and (b) pressure drop across various sized orifice.

at a minimum for better engine efficiency and transient response. Also, according to Liu and Pfeiffer,[6] introducing a pressure drop across the air intake system (AIS) throttle can considerably improve the LP-EGR percentage estimate. Therefore, it is of interest to minimize AIS throttling (and consequently the ΔP across the EGR valve) without sacrificing EGR estimation accuracy. Authors in[10–21,26,27] reviewed the control system strategies to meet Fuel economy with sensor configurations but doesn't address the high pulsating noise in sensor measurements.

Doblhoff et al.[7] reviewed the methods and measurement techniques for steady flow that includes differential pressure flow meters, electromagnetic and ultrasonic flow meters, vortex shedding flowmeters, and hot wire anemometers, but does not propose solutions for higher frequency flow pulsations when they are present. McKee discusses different types of pulsation-induced errors and the use of Square Root Error (SRE), however, Robert does quantify the needs of a fast response transducer that system would be required to measure flow accurately. Nevertheless, some effort has been made by various authors to investigate and establish the use of orifice plates for the measurement of pulsating flow.[22–25]

The objective of this work is to understand the factors that affect EGR mass flow measurement accuracy in the presence of fluctuating pressures. In addition, this work will propose solutions and finally demonstrate the effectiveness of the solutions. This paper investigates the issue of estimating the mass flow rates of pulsating flows, in particular, the difficulty of handling transient, reversing flows across a valve. The current work evaluates the application of different flow estimation methodologies in the estimation of EGR percentage using a ΔP measurement across a flow restriction. Various ΔP measurement characteristics and flow formulations are considered.

The remainder of this paper is organized as follows. EGR mass flow measurement techniques using "Delta pressure over orifice" (DPOO) and "Delta pressure over valve" (DPOV) methods are first discussed. The impact of pressure pulsations on mass flow error (DPOV Testing on a dynamometer) is discussed in the next section. Other factors that affect mass flow measurements accuracies such as flow inertia and gauge line length and placement are investigated. In the solution section, a square root technique is used to improve measurement accuracy and simulation results of the effect of inertia on mass flow errors are discussed. Finally, the findings are summarized in the conclusion section.

Experiment

The following is considered in this section: experimental measurement of mass flow over an orifice, measurement of mass flow over a valve, effects of pressure pulsations on mass flow measurement accuracy, the effect of gauge line length on delta pressure measurement accuracy, and inertia effect on measurement accuracy.

Delta pressure over the orifice

Typically, to measure EGR, a sharp-edged orifice is placed downstream of the EGR valve, pressure taps are placed upstream and downstream of the orifice plate and the pressure drop across the plate is measured. The diameter of the orifice is optimized to minimize the pressure drop at high flow rates but still provides good delta pressure measurement resolution at lower mass flows. As an example of the balancing between good resolution and minimizing pressure drop, consider Figure 2(b). For the small diameter orifice, the slope of the EGR mass flow vs pressure drop is small in the low-pressure region. This indicates that small changes in delta pressure results in small changes in mass flow – a desirable behavior. However, achieving high mass flow rates requires large delta pressure drops. For a large diameter orifice, the slope of the EGR mass flow vs pressure drop is large in the low-pressure region. This indicates that a large flow variation causes a small pressure drop variation – an undesirable behavior. However, achieving high mass flow rates requires only small delta pressure drops. One main drawback of using an orifice is that it creates a second pressure drop, the first being the pressure drop across the EGR poppet valve and the second at the orifice. This second pressure drop reduces the amount of EGR that can be delivered from the exhaust system to the air intake system. Knowing the density of the gas, the orifice area, a discharge coefficient and the pressure drop over the orifice, the steady-state, and incompressible mass flow can be calculated according to equation (1).

$$\dot{m} = C_D A_T \sqrt{2\rho \Delta P} \tag{1}$$

Where

$$\dot{m} = flow\ in \frac{m3}{sec}$$

C_D is the discharge coefficient
ρ is the fluid density in kg/m^3

ΔP is the deltapressure
(Upstream pressure − Downstream pressure)
A_T *is the orifice area*

If the flow is to be considered compressible, the computation is slightly more complicated and is based on the pressure ratio of pressures upstream and downstream of the orifice. If the mass flow is considered compressible, then the flow rate can be calculated according to equation (2)

$$\dot{m} = C_D A_T \frac{P_0}{\sqrt{RT_0}} P_r^{\frac{1}{\gamma}} \left\{ \frac{2\gamma}{\gamma - 1} \left[1 - P_r^{\frac{\gamma-1}{\gamma}} \right] \right\}^{\frac{1}{2}} \tag{2}$$

The pressure ratio $\boldsymbol{P_r}$ is the ratio of the downstream pressure over the upstream pressure and typically $\boldsymbol{P_r} < 1.0$. A pressure ratio greater than unity indicates, if inertia is neglected, that the flow is reversed. The discharge coefficient Cd is a factor that accounts for the difference between the theoretical mass flow and the measured mass flow. The value γ is given by the ratio of specific heat of the air in a constant pressure process Cp to the specific heat of the air in a constant volume process Cv. Equations (1) and (2) are derived through the application of Newton's second law with the assumptions of neglecting inertia effects and incompressible flow (equation (1)) and neglecting inertia with the compressible flow (equation (2)).

Delta pressure over the valve

An alternative to using an orifice plate is to create a pressure drop to measure mass flow across the EGR valve. As the poppet valve lifts, it creates an increasing throat area. The relationship between lift and throat area is given by the formulation in Heywood[8] and shown graphically in Figure 3. Because the valve has a valve lift sensor, the throat area A_t can be calculated and used in equation (2). To determine the discharge coefficient C_d, the valve under study was tested in a flow laboratory in which the delta pressure over the valve is held constant as the valve is opened from completely closed to completely open and the mass flow is accurately measured. The test setup is shown in Figure 4(a) and the results of the calculated discharge coefficient are shown in Figure 4(b). From the results, it was

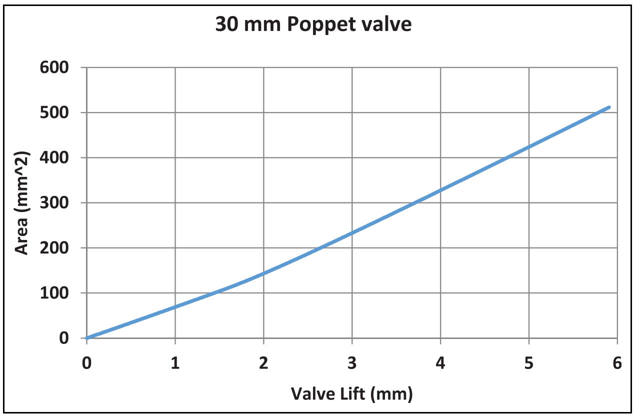

Figure 3. Relationship between lift and throat area for a 30 mm poppet valve.

found that the lift has a strong influence on the discharge coefficient, but the delta pressure has a much weaker influence. For simplicity, the discharge coefficients for several delta pressure are averaged at every lift value and this average C_d as a function of lift is used for the remainder of the analysis.

Effect of pressure pulsations on mass flow error (DPOV testing on dynamometer)

The current technique of measuring the EGR mass flow using the delta pressure over the EGR poppet valve was implemented on a 3.5 L Gasoline Turbocharged Direct Injection (GTDI) engine and a 2.3 L I4 engine. Two engines were used to demonstrate that measurement issues related to pressure pulsations are widespread and not well understood. The delta pressure over the valve was measured using a sensor having a single-pole low pass filter and a corner frequency of 1.5 Hz. The filter is intended to attenuate any noise, including fluctuating pressures, and output the mean delta pressure signal. Several test runs were performed on the two engines in which the engine speed was held constant at 1500 rpm and a load sweep was conducted. Notice that in Figure 1(a) the EGR is routed to the air intake system before the compressor. This arrangement allows the Air Intake System (AIS) throttle to be adjusted to maintain a relatively constant 8 kPa delta pressure over the EGR valve for the 3.5LV6 engine while a constant 4 kPa delta pressure was held for the 2.3 L I4 engine, Because of a lack of understanding of pressure pulsations these constant pressures were used to mitigate the negative effects on measurement accuracy. In both cases, the valve lift was held constant. The plot of mass flow versus engine load is shown in Figure 5.

One thing to notice is that with a constant delta pressure and a constant lift, according to equation (2) the mass flow was expected to be constant as the load is swept (as seen in Figure 1(a) the traditional throttle located just before the engine is used to control engine load). However, this is not the case. As can be seen in Figure 5, as the load increases the mass flow generally

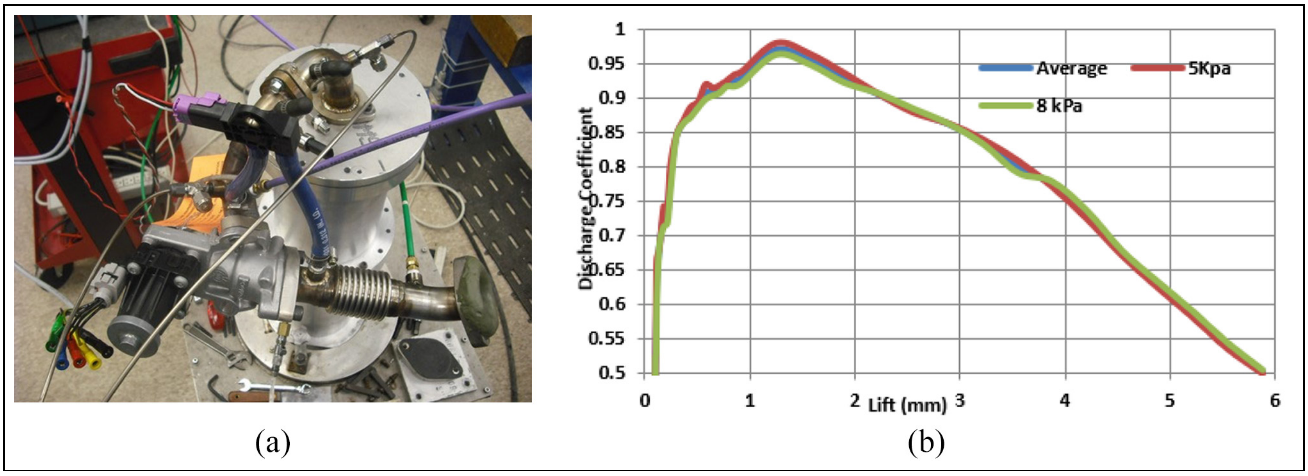

Figure 4. (a) Test setup and (b) discharge coefficient as a function of lift.

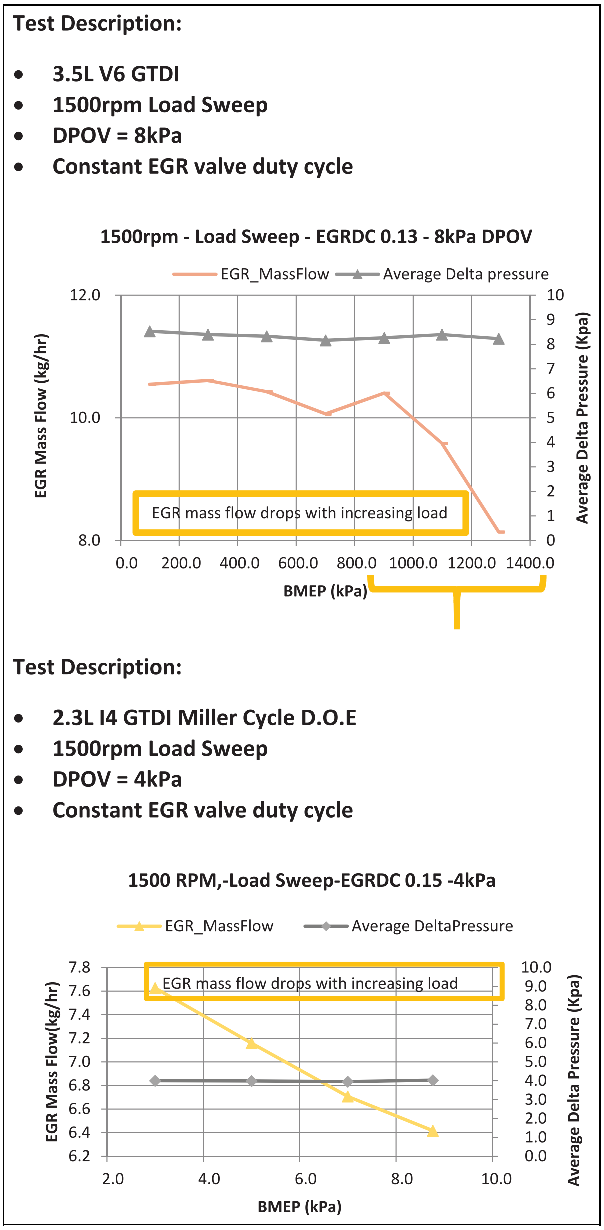

Figure 5. Test results shows mass flow with constant engine RPM, valve lift, and delta pressure and load sweeps.

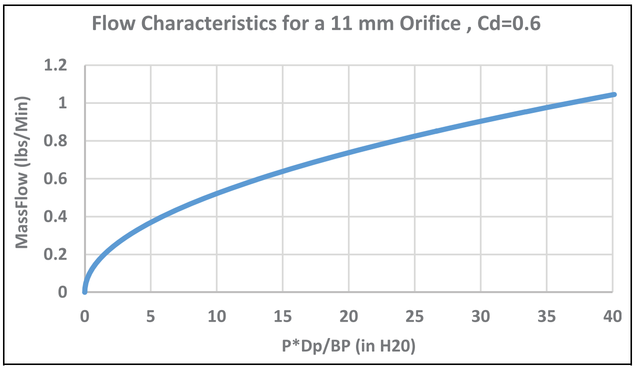

Figure 6. Mass flow as a function of $\rho \times$ Dp normalized by the barometric pressure BP.

falls off. This indicates that there are dynamics associated with the flow that is not being captured and translated to the correct mass flow. A closer investigation into the delta pressure over the valve during the load sweep reveals that there are significant pressure pulsations that exist at the valve. However, the delta pressure sensor was not able to observe these pulsations because of the low pass filter and the low sample rate. For reasons of simplicity assume that the flow is incompressible, therefore, the mass flow is given by equation (1) instead of the compressible flow version given by (2). On a vehicle with an EGR cooler, the temperature is relatively constant and the density of the EGR gas will be mainly dependent on the pressure. Therefore, for a fixed valve lift or an orifice plate with a fixed opening (fixed $C_D A_t$), the mass flow rate is proportional to $\sqrt{2\rho\Delta P}$. This relationship is shown in Figure 6. The x-axis is normalized by the barometric pressure BP.

A delta pressure sensor with a low pass filter that removes pulsation information will output a voltage proportional to the mean delta pressure. If this mean delta pressure is used in equation (1) the average mass flow calculated will be

$$m_{calculated} = C_d A_t \sqrt{2\rho\overline{\Delta P_i}} \tag{3}$$

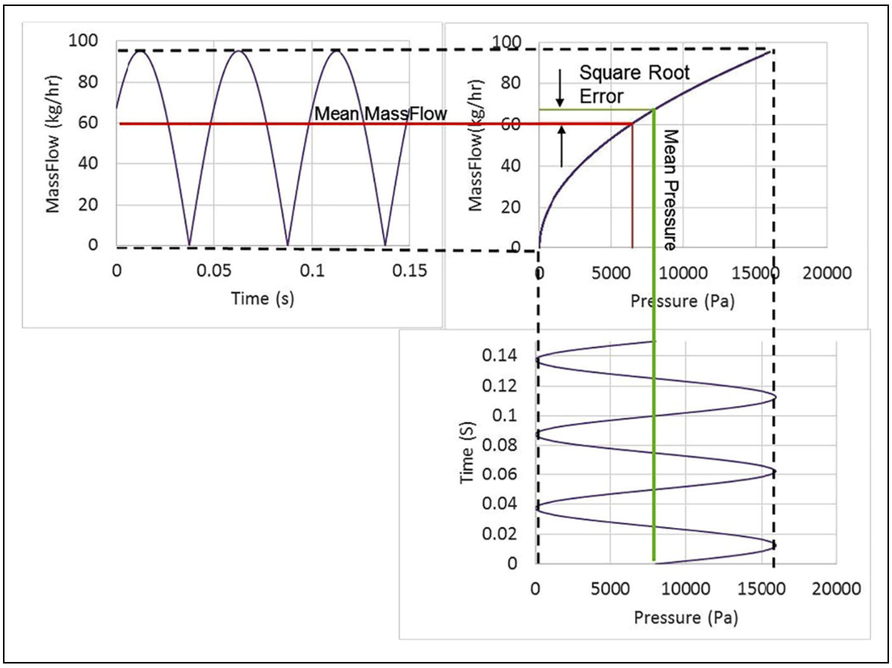

Figure 7. Demonstration of square root error.

This calculation is based on the square root of the average delta pressure. However, this value will be an overestimation of the actual flow which is given by

$$m_{actual} = C_d A_t \sqrt{2\rho \Delta P_i} \tag{4}$$

For this calculation, the actual mass flow is not based on the square root of the average delta pressure but instead on the average of the instantaneous square root of the delta pressure. It is this difference in how the delta pressure is treated that causes the unexpected results in Figure 5. To demonstrate graphically how a slow response sensor causes an error in mass flow calculation, we considered Figure 7. With the assumption of a sinusoidal delta pressure, its mean value applied to equation (4) will result in a mass flow that overestimated the mean mass flow.

The error caused by using a slow responding sensor is called the square root error and is defined as

$$\%SRE = \frac{m_{calculated} - m_{actual}}{m_{actual}} x100 \tag{5}$$

If we assume that the delta pressure is described by

$$Dp(t) = A + bsin(wt + \theta) \tag{6}$$

$$Dp(t)/A = 1 + \frac{b}{A} sin(wt + \theta) \tag{7}$$

Then the % SRE error as a function of the ratio of pulsation amplitude to the mean delta pressure $^b/_A$ is shown in Figure 8. Notice that around $b/A = 1$, the slope of the error curve is rather steep. This indicates that the error quickly grows as the magnitude of the amplitude of the pulsation approaches its mean value.

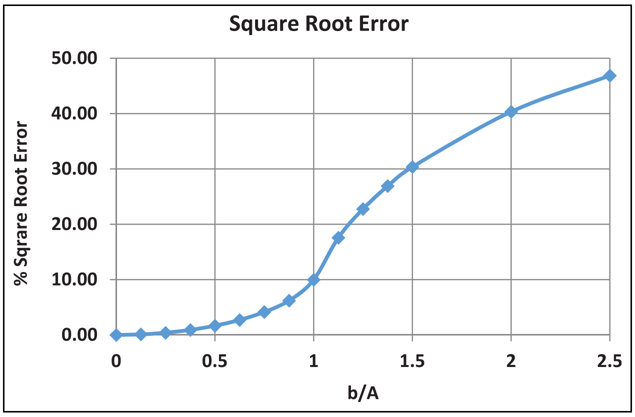

Figure 8. SRE error as a function of normalized delta pressure amplitude.

Just a reduction in 25% of the amplitude ($b/A = 0.75$) will reduce the error by 50%.

This data from Figure 8 indicates that the system needs a delta pressure sensor that has a filter cut-off frequency set high enough to allow observation of the pressure pulsations and a control module that has a data acquisition rate high enough to capture the delta pressure waveform without any aliasing issues. Taking the square root of each sampled delta pressure data point and then averaging these square rooted values will provide the correct mass flow rate as in equation (4).

Effect of inertia on mass flow error

In systems where the flow is not steady but varies as a function of time, the effects of inertia can cause an error

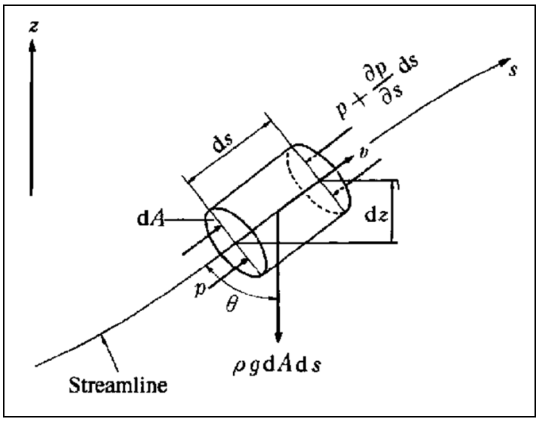

Figure 9. Elemental fluid volume moving along a streamline.

in the proposed technique of determining the mass flow from the high-speed sampling and processing of the delta pressure signal. In the previous discussions, there was no mention of inertia and the assumption was that all the motive force from the delta pressure goes toward mass flow; however, in reality, some of this motive force goes toward accelerating and decelerating the flow in response to the pulsating delta pressure.

Applying Newton's second law of motion to an elemental fluid volume flowing along a streamline shown in Figure 9 results in

$$\rho dAds\frac{dv}{dt} = -dAds\frac{\partial p}{ds} - \rho gdAdScos(\theta) \tag{8}$$

Because this is a one-dimensional flow, the velocity may change with both time and position, that is, $v = v(s, t)$ and a change in velocity can be written as

$$dv = \frac{\partial v}{\partial t}dt + \frac{\partial v}{\partial s}ds$$

where the acceleration is given by

$$\frac{dv}{dt} = \frac{\partial v}{\partial t} + \frac{\partial v}{\partial s}\frac{ds}{dt} = \frac{\partial v}{\partial t} + v\frac{\partial v}{\partial s} \tag{9}$$

Substituting (9) into (8) and assuming that the flow is horizontal so $cos(\theta) = \cos(90) = 0$, then

$$\frac{\partial v}{\partial t} + v\frac{\partial v}{\partial s} + \frac{1}{\rho}\frac{\partial P}{ds} = 0 \tag{10}$$

As shown in Kiwan et al.[9] and repeated here for completeness, for incompressible flow, this leads to

$$K_1\rho\frac{d\dot{m}(t)}{dt} + K_2\dot{m}^2(t) = \rho\Delta P \tag{11}$$

However, if the compressibility of the working fluid is taken into account where the isentropic process $\rho = \rho_0(\frac{P}{P_0})^{\frac{1}{\gamma}}$ is used in (10) then

$$\frac{\partial v}{\partial t} + v\frac{\partial v}{\partial s} + \frac{P_0^{\frac{1}{\gamma}}}{P^{\frac{1}{\gamma}}}\frac{1}{\rho_0}\frac{\partial P}{ds} = 0 \tag{12}$$

Again, as shown in Kiwan et al.[9] this leads to the compressibility form of equation (11) which is

$$\tilde{K}_1(C_DA_t)^2\frac{P_0}{RT_o}P(t)_r^{\frac{2}{\gamma}}\frac{d\dot{m}(t)}{dt} + \dot{m}^2(t) = \left[C_DA_T\frac{P(t)_0}{\sqrt{RT_0}}P(t)_r^{\frac{1}{\gamma}}\left\{\frac{2\gamma}{\gamma-1}\left[1-P(t)_r^{\frac{\gamma-1}{\gamma}}\right]\right\}^{\frac{1}{2}}\right]^2 \tag{13}$$

The effects of inertia are taken into account by the first term on the left-hand side. Notice that the right-hand side of equation (13) is the square of that shown in equation (2).

$$P(t)_r = \frac{P(t)_o - DP(t)}{P(t)_o} \tag{14}$$

For a mass flow measurement system such as that needed for low or high-pressure EGR mass flow measurement, the pressure drop across an orifice should be measured at a sample rate that adequately captures the dynamic behavior of pressure pulsations. A good rule of thumb is to sample at least 10 × the maximum dominant frequency in the pressure signal.

As an example, for a six-cylinder engine in which the EGR is taken from only one bank, at 3500 rpm, the frequency of pulsations on the one bank will be 3500 rpm/60 (s/min) × 6/2 × 0.5 = 87 Hz. Then, an appropriate sample rate will be around 1 k samples/s. In addition to the highly sampled delta pressure signal, the valve lift (*and* C_DA_T) and the upstream pressure is measured. With these pieces of information, everything on the right side of equation (13) is known since $P(t)_o$ is the pressure measured upstream at time t and $P(t)_r$ is shown in equation (14). For a measurement system, the assumption is that the instantaneous value of the right side of equation (13) is equal to the square of the mass flow rate $\dot{m}2(t)$. This treats the flow statically as given by equation (2). However, this assumption neglects the first inertia term on the left side of equation (13) and results in mass flow calculations outside of acceptable levels. The equations here are further used and compared in the 1-D flow simulation software and the results are discussed in the solution section.

Effect of gauge line on the accuracy of delta pressure measurement

To accurately measure the delta pressure pulsations within the EGR tube, care must be taken when assembling the measurement hardware. Whether using a fixed orifice or a valve opening as the pressure drop mechanism, small diameter tubes called gauge lines are installed at taps upstream and downstream of the orifice and are used to communicate the instantaneous pressure within the EGR tube to the delta pressure sensor. However, the length of these gauge lines and the placement of the taps can affect the representation of the pressure within the EGR tube by the delta pressure sensor.

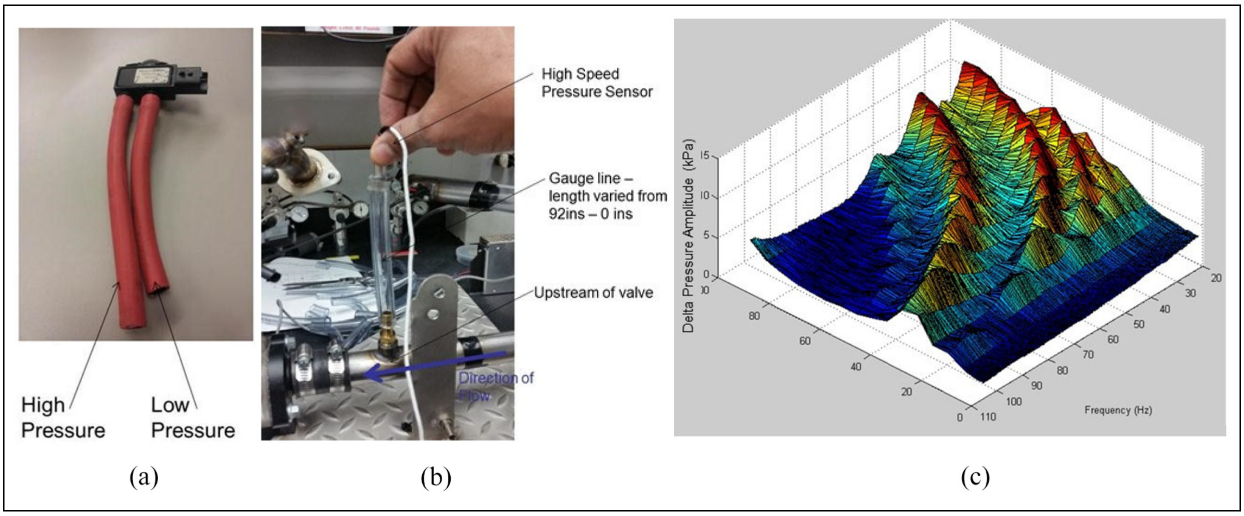

Figure 10. (a) Delta pressure with gauge lines, (b) testing effects of various gauge line lengths on pressure measurement, and (c) frequency induced resonance within gauge lines.

An experiment was conducted to study the effects of gauge line length on the measurement of pressure within an EGR tube. As shown in Figure 10(b), the clear plastic gauge line length was varied between 90 and 0 inches (pressure measured within EGR tube). For a given gauge line length, the pulsation frequency was increased from 20 to 110 Hz and the pressure was measured at the end of the tube. The results are summarized in the 3-D plot in Figure 10(c). It shows that as the gauge lines get longer, resonances occur at lower frequencies causing an amplification of the pressure pulsations within the EGR tube. When these resonant conditions occur, the sensor gives a false representation of the delta pressure within the EGR tube. At gauge line lengths of about 4 inches or less, no resonances occur within the frequency range of engine cylinder firings. In practice, it will be difficult to keep the gauge line length as low as this recommended value because the gauge line is used to reduce the temperature of the EGR gas reaching the sensor to protect it from damage.

A second experiment was conducted in which the location of the upstream and downstream taps was varied and its effect on the delta pressure measurement was recorded. The blue ovals in Figure 11(a) show the upstream locations tested and the yellow ovals show the downstream locations tested. Figure 11(b) shows that as the upstream tap location varies, there are only small changes in the delta pressure readings – the largest changes being at the upper frequencies. Unlike the upstream locations, the downstream locations can have a big effect on the delta pressure reading. If the tap is placed within two diameters of the orifice (blue curve), the delta pressure readings are very different than those places further away from the orifice (green and orange curves) as shown in Figure 11(c). The recommendation would be to place the downstream tap at a minimum of two tube diameters away from the orifice.

Solution

Demonstration of application of square root technique to improve measurement accuracy. As part of a robust EGR mass flow measurement system, the delta pressure sensor output must accurately represent the delta pressure within the EGR Tube. To achieve this, close attention was paid to the mechanics of the measurement system. The gauge lines were kept as short as possible. This avoids the gauge lines from amplifying or attenuating the pressure pulsations at the delta pressure sensor. In addition, the line diameters are kept small at ¼ inch. The tap locations for the high-pressure gauge line are placed one pipe diameter upstream of the orifice and the tap for the low-pressure gauge line are placed at least two diameters downstream of the orifice. As proposed above, to minimize the measurement error due to the square root effect, a fast responding delta pressure sensor was installed across a fixed orifice on a 3.3 L dynamometer engine. To demonstrate the advantage of using a high-speed sensor coupled with high data collection rates over a filtered sensor that was previously used, data was also collected with this slower sensor.

Note that in Figure 12(a) the points indicated in the blue oval are shifted away from the characteristic curve shown in Figure 5. The data taken for this plot used a slow responding sensor whose output voltage was proportional to the mean of the fluctuating delta pressure. The points that are shifted from the expected curve are from operating conditions where the BMEP load > 6 bars. At these loads, the pressure pulsations are large compared to the mean delta pressure and the significant SRE is reflected in the plot. Note that the SRE as demonstrated in Figures 7 and 8 is related to the ratio of the pressure pulsation amplitude relative to the mean pressure and the error is not related to the pulsation frequency. When a faster sensor with a higher sample rate is used and equation (4) is employed, the plot of

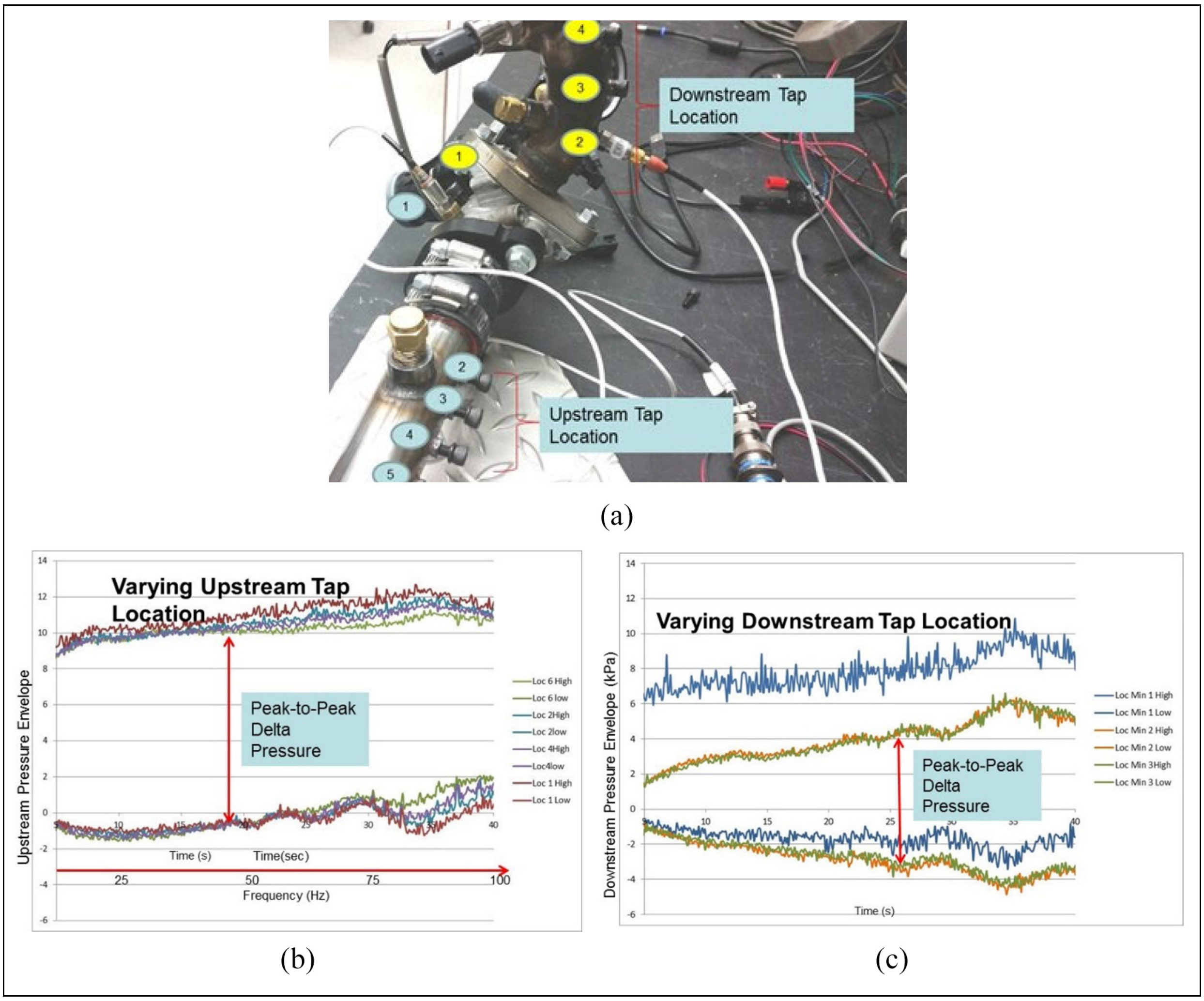

Figure 11. (a) Experiment to investigate effects of tap location, (b) variation in pressure measurement for upstream tap location, and (c) variation in pressure measurement for downstream tap location.

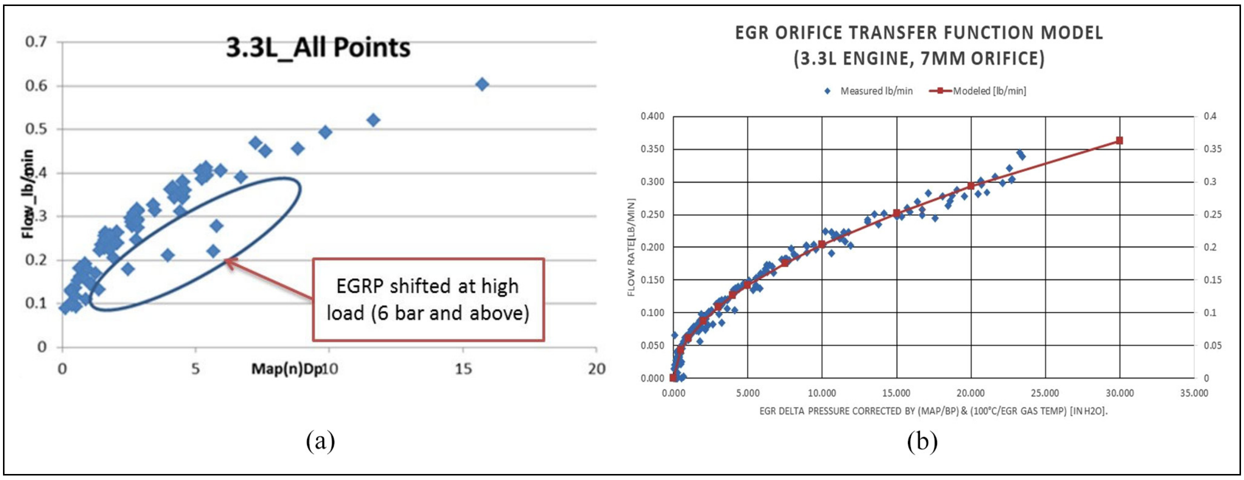

Figure 12. Demonstration of the application of the square root technique to improve measurement accuracy: (a) 3.3l engine flow data with slow responding sensor, (b) EGR Flow data with faster sensor and SRE technique.

Figure 12(b) is obtained. This approach practically eliminated the SRE error and all test points are falling on the expected characteristic curve. The test points here in Figure 12(b) when compared to shifted points in Figure 12(a) showed an improved accuracy by 43% due to the elimination of SRE. The price of this

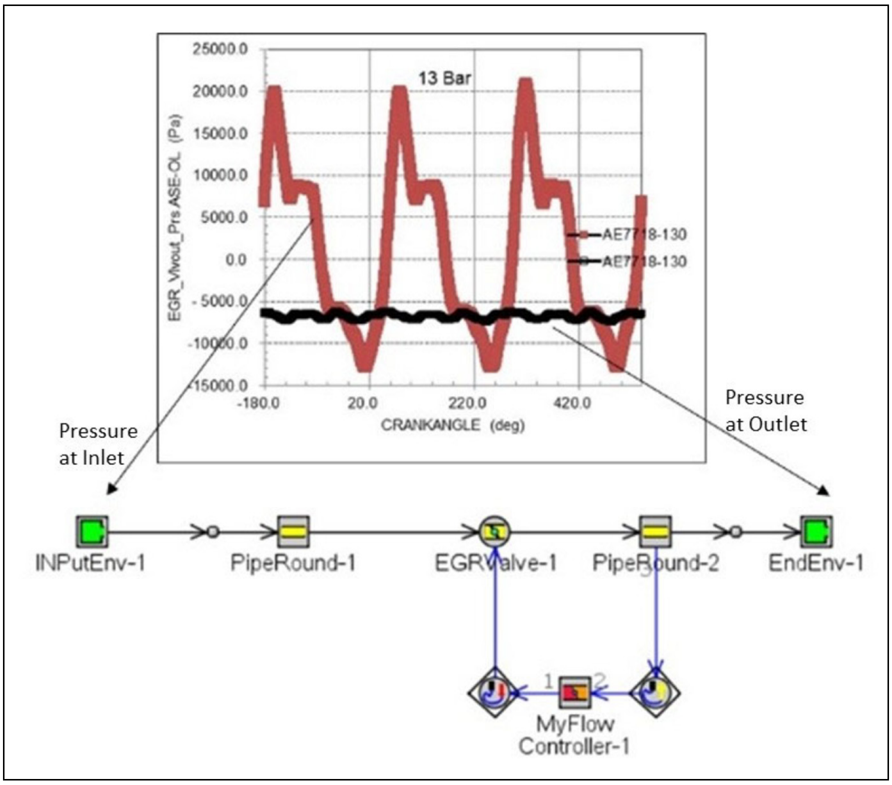

Figure 13. GT-power model used to study the effects of inertia on measurement error.

increased accuracy for calculating the EGR mass flow is more ECM memory to buffer data collected at high sample rates and processing time to calculate the square root of each sampled data point.

Investigation of the effect of inertia on mass flow error. To quantify the error resulting from ignoring the inertia term, a 1-D flow CAE simulation was conducted using GT-Power. The model consists of a 30 mm EGR poppet valve with inlet and outlet pipes. A pulsating pressure profile is imposed at the open end of the inlet pipe and the resulting mass flow through the valve is studied for various delta pressure frequencies, amplitude, and valve lift. This mass flow which will include the effects of inertia is compared to that obtained by the mass flow calculated from just the right side of equation (13). The difference between these two is the mass flow error resulting from a measurement system that doesn't account for inertia.

The GT power model used in the simulation is shown in Figure 13. An example of the pressure profiles imposed on the inlet and the outlet pipes are shown in Figure 14(a). These profiles were obtained from measuring the gauge pressure upstream and downstream of the EGR valve on a 3.5 L GTDI gas engine during dyno testing. The difference between the two pressure profiles will give the delta pressure that drives the gas flow as shown in Figure 14(b).

On close examination of the curve in Figure 14(a), it can be seen that the delta pressure just falls below zero delta pressure. For a measurement system that neglects inertia, the instantaneous mass flow calculated from the instantaneous delta pressure using equation (2) is shown as the blue curve in Figure 14(b). Notice that at the times of slightly negative delta pressures, there is an exaggerated negative mass flow. This is because, as shown in Figure 6, at very low delta pressures, the mass flow vs delta pressure curve is very steep so small changes in delta pressure result in large mass flow. When inertia is considered, the true mass flow is shown as the red curve in Figure 14(b). The difference between the red and blue curves is the measurement error which can be averaged over time or cylinder cycles.

A series of simulations were performed to estimate the range of errors that would occur over various engine speeds and engine loads. Table 1 was obtained from dynamometer testing on the V6 engine and it shows the intake air mass flow for various BMEP ranging from 500 to 1300 kPa and engine speeds from 1000 to 3500 rpm. If it is desired to flow 15% EGR, the EGR mass flow corresponding to each speed/load pair in Table 1 is shown in Table 2. It is these EGR mass flows that must be delivered through the EGR valve under the prevailing delta pressures. The measured delta pressures at the various engine loads are shown in Figure 15.

These delta pressures are applied to the model in Figure 13 and the mass flow curves similar to those in Figure 14(b) were obtained and then the errors in mass flow were calculated. Error curves are obtained for each

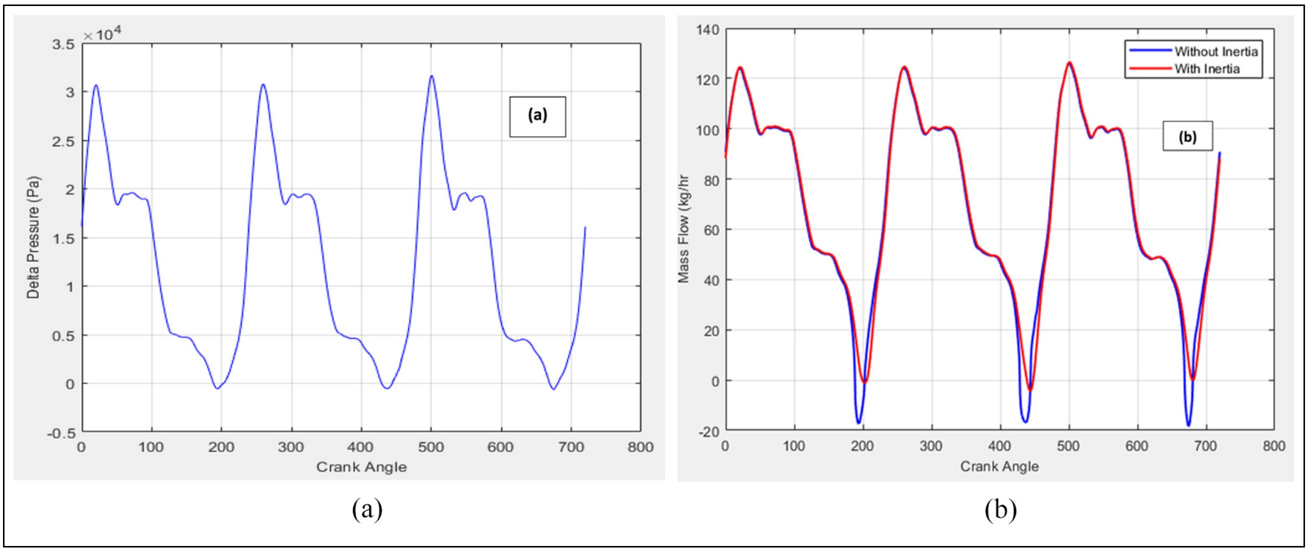

Figure 14. (a) Delta pressure profile and (b) mass flow without taking into account inertia compared to flow that takes into account inertia.

Table 1. Intake air mass flow for various engine loads and engine speeds.

Speed/BMEP	Air Mass flow kg/h				
	500	700	900	1100	1300
1000	53.12	72.34	89.58	93.04	107
1500	78.75	105.21	147.95	162.91	196.27
2000	108.28	145.27	181.8	213.8	255.55
2500	139.5	180.63	227.37	271.28	317.31
3000	169.45	222.92	274.94	325.35	380.94
3500	204.13	265.92	325.12	384.56	446.48

Table 2. EGR mass flow resulting in 15% EGR.

Speed/BMEP	EGR mass flow kg/h				
	500	700	900	1100	1300
1000	9.37	12.76	15.8	16.41	18.88
1500	13.89	18.56	26.1	28.74	34.63
2000	19.1	25.63	32.08	37.72	45.09
2500	24.61	31.87	40.12	47.87	55.99
3000	29.9	39.33	48.51	57.41	67.22
3500	36.02	46.92	57.37	67.86	78.79

load over the simulated speed range. These error curves are shown in Figure 16.

From the error data, it appears that if EGR mass flow is to be calculated using the delta pressure and valve lift and neglecting the effects of inertia by using equation (2), the errors will be conservatively limited to $\pm 1.5\%$. If this falls within the required measurement accuracy, then a measurement technique that samples the delta pressure at a high rate, and applying equation (2) will give a mass flow value that is accurate enough to meet requirements.

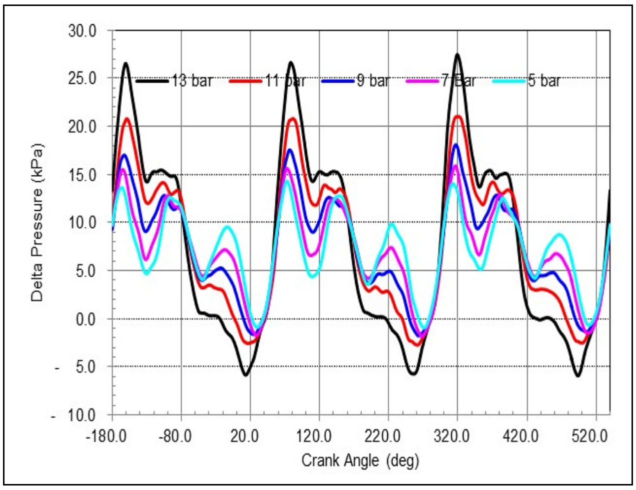

Figure 15. Delta pressures used in simulation for speeds 1000–3500 rpm and loads 500–1300 kPa.

Summary/conclusions

It is necessary to accurately measure EGR mass flow to deliver the requested torque through proper air and fuel management since EGR acts to displace air. To determine the EGR mass flow, the pressure drop across a restriction such as an orifice plate or valve opening is measured using a delta pressure sensor. The work here focuses on the objective of understanding different noise factors associated with EGR mass flow measurement and coming up with solutions that exhibit high measurement accuracy.

1. It was demonstrated that using a slow responding sensor with a low sample rate leads to erroneous mass flow calculation when significant pressure pulsations exist. This is a result of the square root

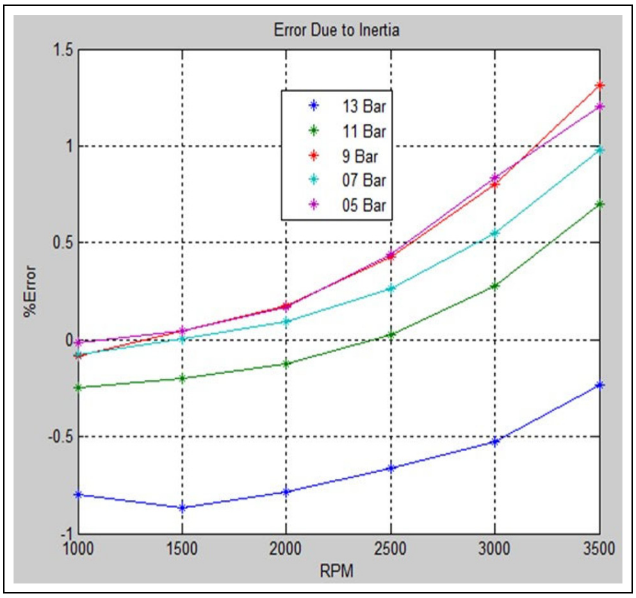

Figure 16. EGR mass flow measurement error for various engine speeds and engine loads.

relationship between the delta pressure and mass flow.

2. Significant pressure pulsations across the EGR valve typical of HP-EGR configurations result in % EGR estimation errors in estimated EGR percentage that can be as high as 50% when the steady compressible orifice equation is used with a cycled-averaged ΔP measurement on gasoline engines.
3. The proposed solution to mitigate the square root error is to use a fast responding delta pressure sensor that captures the dynamics of the pressure pulsations and sample the sensor output at a high enough sample rate that avoids the aliasing. The data should not be processed using equation (3) and typically done but it should be processed using equation (4). This reduces the Square Root Error and reduces the need to maintain a given mean delta pressure over the valve. In addition, the gauge line lengths should be kept as short as possible to establish resonance frequencies outside of the operating range. Lastly, the downstream tap for the delta pressure sensor should be a minimum of two EGR tube diameters away from the flow restriction.
4. The penalty for implementing the proposed solution is the use of more memory and computing time to perform the square root operation on each sampled data.
5. It was also demonstrated that for the 3.5 L GTDI gas engine tested, neglecting the effects of flow inertia results conservatively in a ±1.5% error in the mass flow calculation.
6. This method is validated on production vehicles and has shown excellent results in meeting scheduled steady-state EGR delivery centered within ±1.0% MOS (Measure of Success).

Declaration of conflicting interests

The author(s) declared no potential conflicts of interest with respect to the research, authorship, and/or publication of this article.

Funding

The author(s) received no financial support for the research, authorship, and/or publication of this article.

ORCID iD

Sumanth Reddy Dadam https://orcid.org/0000-0002-9045-5310

References

1. Westin F, Grandin B and Ångström HE. The influence of residual gases on knock in turbocharged SI-engines. *SAE technical paper* 2000-01-2840, 2000.
2. Teodosio L, De Bellis V and Bozza F. Fuel economy improvement and knock tendency reduction of a downsized turbocharged engine at full load operations through a low-pressure EGR system. *SAE technical paper* 2015-01-1244, 2015.
3. Potteau S, Lutz P, Leroux S, Moroz S and Tomas E. Cooled EGR for a turbo SI engine to reduce knocking and fuel consumption. *SAE technical paper* 2007-01-3978, 2007.
4. Alger T, Chauvet T and Dimitrova Z. Synergies between high EGR operation and GDI systems. SAE technical paper 2008-01-0134, 2008.
5. Zhong L, Musial M, Reese R and Black G. EGR systems evaluation in turbocharged engines. *SAE technical paper* 2013-01-0936, 2013.
6. Liu F and Pfeiffer J. Estimation algorithms for low pressure cooled EGR in spark-ignition engines. *SAE Int J Engines* 2015; 8(4): 1652–1659.
7. Doblhoff-Dier K, Kudlaty K, Wiesinger M and Gröschl M. Time resolved measurement of pulsating flow using orifices. *Flow Meas Instrum* 2011; 22: 97–103.
8. Heywood JB. *Internal combustion engine fundamentals*. New York: McGraw-Hill, 1988.
9. Kiwan R, Stefanopoulou AG, Martz J, Surnilla G, Ali I and Joseph Styles D. Effects of differential pressure measurement characteristics on low pressure-EGR estimation error in Si-engines. *IFAC-PapersOnLine* 2016; 49(11): 722–729.
10. Giechaskiel B, Joshi A, Ntziachristos L and Dilara P. European regulatory framework and particulate matter emissions of gasoline light-duty vehicles: a review. *Catalysts* 2019; 9: 586.
11. Van Nieuwstadt MJ. *Pressure sensor diagnosis via a computer*. Patent US6947831B2, USA, 2003
12. Lambert CK, Bumbaroska M, Dobson D, Hangas J, Pakko J and Tennison P. Analysis of high mileage gasoline exhaust particle filters. *SAE Int J Engines* 2016; 9(2): 1296–1304.
13. Van Nieuwstadt M and Ulrey J. Control strategies for gasoline particulate filters. *SAE technical paper* 2017-01-0931, 2017.
14. Richter JM, Klingmann R, Spiess S and Wong KF. Application of catalyzed gasoline particulate filters to GDI vehicles. *SAE Int J Engines* 2012; 5(3): 1361–1370.

15. Chan TW, Meloche E, Kubsh J, Rosenblatt D, Brezny R and Rideout G. Evaluation of a gasoline particulate filter to reduce particle emissions from a gasoline direct injection vehicle. *SAE Int J Fuel Lubricants* 2012; 5(3): 1277–1290.
16. Sappok A, Wang Y, Wang RQ, Kamp C and Wong V. Theoretical and experimental analysis of ash accumulation and mobility in ceramic exhaust particulate filters and potential for improved ash management. *SAE Int J Fuel Lubricants* 2014; 7(2): 511–524.
17. Dadam S, Sharma S and Jentz RR. *Method for variable position exhaust tuning valve diagnostics*. Patent 10844762, USA, 2020.
18. Dadam SR, Jentz R, lenzen T and Meissner H. Diagnostic evaluation of exhaust Gas recirculation (EGR) system on gasoline electric hybrid vehicle. *SAE technical paper* 2020-01-0902, 2020.
19. Van Nieuwstadt MJ, Lehmen A, Martin D, Eric Rollinger J, Dadam S and Bhat R. *Gasoline particulate filter diagnostics*. Patent 10323562, USA, 2019.
20. Jentz R, Lenzen T, Dadam S, Meissner H and Hancock K. *Method and system for exhaust gas recirculation system diagnostics*. Patent 10632988, USA, 2020.
21. Jentz R, Sharma R and Dadam S. *Heat exchanger for exhaust tuning systems*. Patent 10436087, USA, 2019.
22. Alger T, Gingrich J, Roberts C and Mangold B. Cooled exhaust-gas recirculation for fuel economy and emissions improvement in gasoline engines. *Int J Engine Res* 2011; 12(3): 252–264.
23. Galindo J, Dolz V, Monsalve-Serrano J, Bernal MA and Odillard L. Impacts of the exhaust gas recirculation (EGR) combined with the regeneration mode in a compression ignition diesel engine operating at cold conditions. *Int J Engine Res* 2021; 14680874211013 986.
24. Galindo J, Climent H, Navarro R, Miguel-García J, Chalet D and Pretot PE. A study on the high pressure EGR transport and application to the dispersion among cylinders in automotive engines. *Int J Engine Res* 2021; 22: 3164–3178.
25. Galindo J, Climent H, Navarro R and García-Olivas G. Assessment of the numerical and experimental methodology to predict EGR cylinder-to-cylinder dispersion and pollutant emissions. *Int J Engine Res* 2021; 22: 3128–3146.
26. Reitz RD, Ogawa H, Payri R, et al. IJER editorial: the future of the internal combustion engine. *Int J Engine Res* 2020; 21: 3–10.
27. Macián V, Luján JM, Climent H, Miguel-García J, Guilain S and Boubennec R. Cylinder-to-cylinder high-pressure exhaust gas recirculation dispersion effect on opacity and NOx emissions in a diesel automotive engine. *Int J Engine Res* 2021; 22(4): 1154–1165.